Elsevier Editorial System(tm) for International Journal for Parasitology
Manuscript Draft

Manuscript Number: IJPara14_460R1

Title: Biogenesis of the crystalloid organelle in Plasmodium involves microtubule-dependent vesicle transport and assembly

Article Type: Full Length Article

Keywords: Plasmodium berghei; vesicle transport; organellogenesis; LCCL protein

Corresponding Author: Dr. Johannes Dessens, PhD

Corresponding Author's Institution: London School of Hygiene and Tropical Medicine

First Author: Sadia Saeed, PhD

Order of Authors: Sadia Saeed, PhD; Annie Z Tremp, PhD; Johannes Dessens, PhD

Manuscript Region of Origin: UNITED KINGDOM

Abstract: Malaria parasites possess unique subcellular structures and organelles. One of these is the crystalloid, a multivesicular organelle that forms during the parasite's development in vector mosquitoes. The formation and function of these organelles remain poorly understood. A family of six conserved and modular proteins named LCCL-lectin adhesive-like proteins (LAPs), which have essential roles in sporozoite transmission, localise to the crystalloids. In this study we analyze crystalloid formation using transgenic Plasmodium berghei parasites expressing GFP-tagged LAP3. We show that deletion of the LCCL domain from LAP3 causes retarded crystalloid development, while knockout of LAP3 prevents formation of the organelle. Our data reveal that the process of crystalloid formation involves active relocation of ER-derived vesicles to common assembly points via microtubule-dependent transport. Inhibition of microtubule-dependent cargo transport disrupts this process and part replicates the LCCL domain deletion mutant phenotype in wildtype parasites. These findings provide the first clear insight into crystalloid biogenesis, demonstrating a fundamental role for the LAP family in this process, and identifying the crystalloid and its formation as potential targets for malaria transmission control.

Dear Prof. Cooke

Thank you very much for reconsidering our manuscript IJPara14_460 for publication. Please find below our response to the Reviewers' and your own comments, including those corresponded in your email of February 1st, 2015. I hope that the revised version now meets with your approval.

Yours sincerely,
Hans Dessens
Corresponding author

Reviewer #2: This resubmission addresses some of the concerns with the original submitted manuscript. Several outstanding issues remain:

*there is insufficient data to describe the newly included "viability assays". In a different section the authors refer to a viability assay described by Al-Khattaf et al (who use propidium iodide to measure accessibility of stain after an osmotic shock), but measuring osmotic lysis is quite different to measuring whether a drug causes some kind of inhibition. No details are given on time periods - is the PI staining done at 24 hours post drug addition? Please add a few more details here for a reader to understand what was scored.
More details on the cell viability assay have been added to the Materials & Methods section (lines 140-143). We have also added in the Results section that ookinete viability was determined at 24h post-gametogenesis (line 294). In addition to the viability assay, the TEM data in Fig. 6 clearly show normal development of subcellular structures and organelles. Thus we have no evidence for cytotoxicity of the inhibitor. Indeed, the reviewer agrees with this in his documented response (your email dated 01 Feb 2015).

*new material has been included to show co-localisation with a commercial ER stain. This staining of this ER-ID marker looks most unlike any previous staining or immunolabeling of Plasmodium ER that I have seen, and appears to occupy most of the volume of the cell. What work has been done to validate that this commercial marker indeed accurately labels the Plasmodium ER - there are several good Plasmodium ER antibodies available for testing.
This reviewer appears not very familiar with *P. berghei* sexual stage cell biology. It is important to keep in mind that LAP3 is expressed only in female gametocytes. The *P. berghei* female gametocyte is known for having extensive ER that in TEM is shown to occupy a large area of extranuclear cytoplasm (e.g. Fig. 2A, Olivieri et al 2015, Cell Microbiol 17:355-368). This fits very well with the distribution of LAP3::GFP-based fluorescence in live LAP3/GFP gametocytes (e.g. Fig. 2B, Saeed et al 2012, MBP 185: 170-173), and that of ER tracker and the ER protein SHLP1 in *P. berghei* gametocytes (Fig. S1B, Patzewitz et al 2013, Cell Rep 3:622-629). We have also added new immunogold EM data of LAP3/GFP gametocytes, which shows labelling of a large and distinct area of extranuclear cytoplasm (Fig. 1B). The relatively harsh fixation protocol required for optimal antibody binding poorly preserves the subcellular structures, precluding a definitive allocation of the label to the ER. Nonetheless, the distribution of the gold particles is consistent with the other observations of ER in female *P. berghei* gametocytes as mentioned. This has been added to the relevant part of the Results section (lines 201-206). In addition, details on the IEM protocol used have been added to the Materials & Methods section (lines 185-187).

Indeed, in his documented response (part of your email of 01 Feb 2015) reviewer 2 agrees that the ER structure identified by Patzewitz could be the same as the structure we observe in Fig 1C. However, the reviewer still questions the much smaller ER structure that is identified by BiP staining in a *P. berghei* gametocyte in the paper from Pace et al., 2006 in Molecular Microbiology. This discrepancy can be easily explained by the fact that the Pace et al study shows a male gametocyte (because BiP in this study is used as a counter stain for the male gametocyte-expressed nuclear

protein SET). In contrast to females, male gametocytes are known to possess a larger nucleus and very limited ER.

The likely ER localisation of LAP3 in the female gametocyte and during the early part of ookinete development is strongly supported by the fact that LAP3 possesses a canonical ER signal peptide, and by the observed co-localisation of LAP3 with commercial ER stain (Fig. 1C). Indeed, in his documented response (your email of 01 Feb 2015) the reviewer agrees with this concept (i.e. that LAP3 is trafficked via the ER), but expresses surprise at the length of time that this protein remains in the ER, and suggests that we show some slightly older parasites where the labelling has started to become more punctate.
Response: Not enough is known about *Plasmodium* sexual stage cell biology to make assumptions about how long trafficking through the ER should take. What we do know is that LAP3 exits from the ER, since it relocates very efficiently to the ookinete crystalloids. The time course of crystalloid/ookinete development in our manuscript does in fact already show 'older' parasites where the LAP3::GFP distribution is becoming more punctate before crystalloid assembly becomes evident (Fig.1A, 6h), which could point to its accumulation around ER exit sites. We now point this out specifically in the relevant Results section (lines 210-212).

*The remainder of the western blot has now been included in 2C, which demonstrates considerable labelling of bands of unanticipated size. It is very disappointing that the original blots had been cropped to remove these additional bands.
It is important to keep in mind that the original western served only to show the size difference of full-length LAP3::GFP with (lane 2) and without (lane 3) the LCCL domain, which it achieved effectively. This is why the western was originally cropped, so not to detract from this issue with the other bands. Indeed, the reviewer now agrees in his documented response (your email of Feb 2015) that this was a valid reason for cropping
The authors explain the major unexpected fraction as being a cross reacting host protein but no data are included to support this, and the band disappears in the LCCL domain-knockout, which is not consistent with this interpretation. I am not familiar with other papers reporting major cross reacting bands in Plasmodium using commercial antibodies to GFP. More work is needed here to adequately explain what is going on with these different protein forms.
There is only one obvious non-specific band that is recognised by the GFP antibodies, of about 65K (Fig. 2C, marked with asterisk). The non-specificity is highlighted by its presence in a wildtype parasite control (lane 1, Fig 2C). Several other papers have reported the presence of this cross-reactive protein (e.g. Fig. 2A, Saeed et al., 2012, MBP 185:170-173; Fig. 5C, Tremp et al., 2013, Mol Micro 89:552-564). This was already pointed out in the legend of Fig. 2 (lines 589-596). We also explained the presence of the small amount of GFP cleavage in the revised manuscript (lines 241-243). Thus the presence of the additional bands on the blot are adequately explained.

*The annotation of the supposed hemozoin crystals in 3B and 4C, is still inconsistent and unconvincing. Some of the objects shown are surrounded single, double or no membranes, and some are electron dense while others are electron lucent. It is insufficient justification to claim that "we know from experience very well what to look for". If the apparent association of the mini-crystalloids with hemozoin is not

obvious in panels that are presented as figures, it is hard to expect that we should simply accept claims of association based on experience.

It has been well documented (as early as 1969) that crystalloids associate with pigment, and you can clearly see this also in some of the bright field images. More importantly, whether pigment is there or not is in a sense trivial: it does not change the main finding of this study, namely, that crystalloids are formed by a process of vesicle assembly that involves microtubule-dependent transport. In his documented response (your email of Feb 1, 2015) the reviewer remains of the opinion that the presence of hemozoin crystals is not demonstrated conclusively, and suggests that we can modify the manuscript without weakening it by removing the claim of persistence of association. Accordingly, we have removed all claims of association of hemozoin with crystalloids from the Results and Discussion sections of the manuscript. In addition, the relevant figures and legends have also been modified by removing hemozoin annotation.

***Graphical Abstract (for review)**

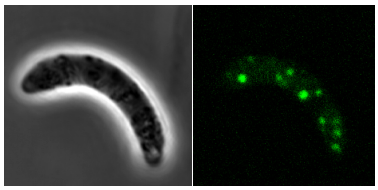

***Highlights (for review)**

- Crystalloid formation occurs during the early part of ookinete development
- Deletion of the LCCL domain of PbLAP3 causes delayed crystalloid formation
- Knockout of PbLAP3 prevents crystalloid formation altogether
- Crystalloid biogenesis involves active vesicle transport and assembly
- Crystalloid assembly is microtubule-dependent

Biogenesis of the crystalloid organelle in *Plasmodium* involves microtubule-dependent vesicle transport and assembly

Sadia Saeed, Annie Z. Tremp and Johannes T. Dessens*

Pathogen Molecular Biology Department, Faculty of Infectious and Tropical Diseases, London School of Hygiene & Tropical Medicine, Keppel Street, London WC1E 7HT, United Kingdom

*Author for correspondence: Johannes T. Dessens, Pathogen Molecular Biology Department, Faculty of Infectious and Tropical Diseases, London School of Hygiene & Tropical Medicine, Keppel Street, London WC1E 7HT, United Kingdom. Tel.: +44 207 9272865; Email: Johannes.Dessens@lshtm.ac.uk

Abstract

Malaria parasites possess unique subcellular structures and organelles. One of these is the crystalloid, a multivesicular organelle that forms during the parasite's development in vector mosquitoes. The formation and function of these organelles remain poorly understood. A family of six conserved and modular proteins named LCCL-lectin adhesive-like proteins (LAPs), which have essential roles in sporozoite transmission, localise to the crystalloids. In this study we analyze crystalloid formation using transgenic *Plasmodium berghei* parasites expressing GFP-tagged LAP3. We show that deletion of the LCCL domain from LAP3 causes retarded crystalloid development, while knockout of LAP3 prevents formation of the organelle. Our data reveal that the process of crystalloid formation involves active relocation of ER-derived vesicles to common assembly points via microtubule-dependent transport. Inhibition of microtubule-dependent cargo transport disrupts this process and replicates the LCCL domain deletion mutant phenotype in wildtype parasites. These findings provide the first clear insight into crystalloid biogenesis, demonstrating a fundamental role for the LAP family in this process, and identifying the crystalloid and its formation as potential targets for malaria transmission control.

Keywords: crystalloid; cargo transport; LCCL protein; transgenic parasite

1. Introduction

Reducing parasite transmission by mosquitoes is an essential part of successful malaria control and eradication programmes. Malaria transmission starts with the uptake of the sexual stages (gametocytes) with the blood meal of a feeding vector mosquito, which initiates rapid gametogenesis and fertilization. The resulting zygotes transform over a 16-24h period into motile elongated stages called ookinetes, which cross the midgut epithelium of the insect and then round up and transform into oocysts. In the ensuing 2-3 weeks, the oocysts grow and differentiate to generate thousands of progeny sporozoites. After egress from the oocysts, the sporozoites invade and inhabit the salivary glands, and are transmitted to new hosts by mosquito bite to initiate new malaria infections.

Plasmodium crystalloids are transient parasite organelles that are uniquely found in ookinetes and young oocysts (Dessens et al., 2011). The organelles have been identified in human, monkey, rodent and bird malaria species, appearing in transmission electron microscopy (TEM) as clusters, 0.5 - 2.0 μm in diameter, of small spherical subunits. These subunits, 35-55 nm in diameter, have been shown in high-resolution TEM to be individually bound by a lipid bilayer, indicating that they constitute small vesicles (Garnham et al., 1962; Garnham et al., 1969; Trefiak and Desser, 1973; Terzakis et al., 1976; Meis and Ponnudurai, 1987). In rodent malaria species, crystalloids are associated with larger vesicles containing hemozoin (also known as the malaria pigment, a product of heme detoxification in the food vacuoles) (Garnham et al., 1969; Sinden et al., 1985; Carter et al., 2008).

Thus far, the only parasite proteins found to localise to crystalloids are a family of six gametocyte-expressed proteins named LCCL-lectin adhesive-like proteins (LAPs) (Carter et al., 2008; Saeed et al., 2010, 2013). LAPs are highly conserved between *Plasmodium* species and possess a modular architecture comprised of multiple domains implicated in protein, lipid and carbohydrate binding (Claudianos et al., 2002; Delrieu et al., 2002; Pradel et al., 2004; Trueman et al., 2004). LAPs were named after the 'LCCL' (*Limulus* clotting factor C and lung gestation protein

71 1) domain (Trexler et al., 2000), which is present in single or multiple copies in all but one family
72 member. In addition, the LAPs possess an amino-terminal ER signal peptide. *Plasmodium* LAPs are
73 predominantly expressed in female gametocytes and, following gametogenesis and fertilization,
74 they efficiently redistribute from the ER to the crystalloids during ookinete development and are
75 subsequently carried over to the young oocyst with the organelles (Carter et al., 2008; Saeed et al.,
76 2010, 2013). Based on available genome data, LAPs appear to be conserved across Apicomplexa,
77 albeit with some variation in the repertoire of LAP family members between genera (Claudianos et
78 al., 2002; Dessens et al., 2004; Lavazec et al., 2009). The uniqueness, complexity and conservation
79 of the LAP architectures strongly suggest that these proteins possess orthologous functions
80 (Lavazec et al., 2009). By contrast, although some genera such as *Cryptosporidium* and
81 *Cystoisospora* possess crystalloid-like structures, crystalloids appear not to be generally conserved
82 in the Apicomplexa. A link between LAPs and crystalloids outside the genus *Plasmodium* is
83 therefore not apparent. There is strong evidence that the *Plasmodium* LAPs are involved in
84 sporozoite transmission: knockout of five of the family members in *P. berghei*, either as single or
85 double knockouts, gives rise to arrested sporozoite development in the oocyst and subsequent
86 failure of the parasite to be transmitted by mosquito bite (Claudianos et al., 2002; Raine et al., 2007;
87 Carter et al., 2008; Ecker et al., 2008; Lavazec et al., 2009). In *P. falciparum* is has been shown that
88 knockout of LAP1 (*Pf*CCp3) and LAP4 (*Pf*CCp2) results in loss of sporozoite transmission (Pradel
89 et al., 2004). Several studies have furthermore shown that the LAPs interact with each other, and
90 are interdependent for correct folding and stability (Pradel et al., 2006; Simon et al., 2009; Saeed et
91 al., 2012), indication that they operate as a protein complex.
92 Within several hours of fertilization, spherical *Plasmodium* zygotes undergo DNA
93 replication followed by meiotic division (Sinden et al., 1985; Janse et al., 1986). During meiosis,
94 spindle microtubules form in the intact nucleus, which are organized from spindle pole plaques
95 embedded in the nuclear membrane (Sinden et al., 1985). The apical complex, initially consisting of
96 two polar rings, is formed under the zygote surface and goes on to form a protrusion. As zygote-to-

97 ookinete transformation advances, this protrusion increases in size at the expense of the spherical
98 progenitor zygote, ultimately forming the mature, banana-shaped ookinete typically by 18-20h post-
99 fertilization (Aikawa et al., 1984; Sinden et al., 1985). Intermediate stages (i.e. part sherical zygote,
100 part elongated ookinete) are known as retorts. Concurrent with the formation of the apical
101 protrusion, a unique cortical structure forms at the site where the protrusion extends from the zygote.
102 This structure, known as the pellicle, is composed of the plasma membrane; an underlying double
103 membrane structure called inner membrane complex; and a cytoskeletal network of intermediate
104 filaments termed subpellicular network (Mann and Beckers, 2001; Morrissette and Sibley, 2002;
105 Khater et al., 2004). Underlying the pellicle are subpellicular microtubules that originate at the polar
106 rings and extend toward the posterior end of the ookinete (Aikawa et al., 1984; Sinden et al., 1985;
107 Morrissette and Sibley, 2002). Besides subpellicular and spindle pole microtubules, cytoplasmic
108 microtubules that appear to originate from at least two cytoplasmic centrioles have been observed in
109 *Plasmodium* zygotes (Aikawa et al., 1984).
110 To date, virtually nothing is known about how crystalloids are formed. In this study, we use
111 LAP3 in the rodent malaria parasite species *P. berghei* (PBANKA_020450) to carry out a detailed
112 study of crystalloid formation. The results obtained provide unique new insight into the processes
113 underlying crystalloid biogenesis, and identify a clear functional relationship between LAP
114 expression, crystalloid formation and sporozoite transmission of malaria parasites. Our data also
115 point to a prominent role of microtubules in crystalloid genesis. The biological significance of these
116 findings with respect to LAP function in apicomplexan parasites is discussed.
117

2. Materials and Methods

2.1 Animal use

All laboratory animal work undergoes regular ethical review by the London School of Hygiene & Tropical Medicine, and has been approved by the United Kingdom Home Office. Work was carried out in accordance with the United Kingdom Animals (Scientific Procedures) Act 1986 implementing European Directive 2010/63 for the protection of animals used for experimental purposes. Experiments were conducted in 6-8 weeks old female CD1 mice, specific pathogen free and maintained in filter cages. Animal welfare was assessed daily and animals were humanely killed upon reaching experimental or clinical endpoints. Mice were infected with parasites suspended in RPMI or PBS by intraperitoneal injection, or by infected mosquito bite on anaesthetized animals. Parasitemia was monitored regularly by collecting of a small volume of blood from a superficial tail vein. Drugs were administered by intraperitoneal injection or where possible were supplied in drinking water. Parasitized blood was harvested by cardiac bleed under general anaesthesia without recovery.

2.2 Parasite maintenance, culture and transmission

P. berghei ANKA clone 234 parasites were maintained as cryopreserved stabilates or by mechanical blood passage and regular mosquito transmission. To purify parasites for genomic DNA extraction, white blood cells were removed from parasitemic blood by passage through CF11 columns. Ookinete cultures were set up overnight from gametocytemic blood (Arai et al., 2001). Mosquito infection and transmission assays were as described using *Anopheles stephensi* (Dessens et al., 1999; Khater et al., 2004) and infected insects were maintained at 20°C at approximately 70% relative humidity. Cell viability assays based on propidium iodide exclusion were carried out as described (Al-Khattaf et al., 2015). Briefly, cell viability was scored by fluorescence microscopy in the presence of 5 ml/L propidium iodide and 1% Hoechst 33258. Ookinetes whose nucleus stained

positive for both propidium iodide and Hoechst were scored as non-viable, whereas ookinetes whose nucleus only stained positive for Hoechst were scored as viable.

2.3 Generation and genomic analysis of transgenic parasite lines

Plasmid pLP-*Pb*LAP3/EFGP (Saeed et al., 2010) served as a template for inverse PCR using primers LAP3-KO-F (ATTCAAAAAGCTTAGGGGCCCTCAT) and LAP3-KO-R (CCTAAGCTTTTTGAATATATTAAAATGGTTGTAATAACCA). The amplified plasmid DNA was circularised via In-Fusion cloning (Takara Bio), resulting in the transfection construct pLP-*Pb*LAP3-KO, in which all but the first 21 codons of *pblap3* have been removed. The same was done with primers LAP3-LCCLKO-F (ACCATCATCCTTTATATTACTCAATACCAAATAGCTATTCA) and LAP3-LCCLKO-R2 (TATAAAGGATGATGGTTCATATATTCATTATCTATTATATTACATGA) to generate the transfection construct pLP-PbLAP3/LCCL-KO, in which the entire LCCL domain, corresponding to amino acids 708 to 846 of *Pb*LAP3, has been removed from the *Pb*LAP3 coding sequence. Plasmids were linearized with *Hin*dIII and *Sac*II to remove the vector backbone, and transfected into purified schizonts as described (Janse et al., 2006). Transgenic parasite lines were obtained by pyrimethamine selection followed by limiting dilution cloning as described (Janse et al., 2006). Genomic DNA extraction and Southern blot were performed as previously described (Dessens et al., 1999). All clonal transgenic parasite populations were checked for the absence of wildtype parasites by diagnostic PCR with primers pDNR-LAP3-F (ACGAAGTTATCAGTCGAGGTACCTAGCGGAAACAACAATGTTC) and LAP3-3'R (CCTCAAGATAGTTACGAATTTAAC).

2.4 Western blot

Parasite samples were heated directly in SDS-PAGE loading buffer at 70ºC for 10 min. Proteins were fractionated by electrophoresis through NuPage 4-12% Bis-Tris precast gels (Invitrogen) and transferred to PVDF membrane according to the manufacturer's instructions. Membranes were blocked for non-specific binding in PBS supplemented with 0.1% Tween 20 and 5% skimmed milk for 1h at room temperature. Goat polyclonal antibody to GFP conjugated to horse radish peroxidase (Abcam ab6663) diluted 1:5000 was applied to the membrane for 1h at room temperature. After washing, signal was detected by chemilluminescence (Pierce ECL western blotting substrate) according to manufacturer's instructions.

2.5 Microscopy

For assessment of fluorescence, live parasite samples were assessed, and images captured, on a Zeiss LSM510 confocal microscope. ER-ID Red (Enzo Life Sciences) was used to stain endoplasmic reticulum according to manufacturer's instructions. Parasites were prepared for electron microscopy by overnight fixation in 2.5% glutaraldehyde/2.5% paraformaldehyde/0.1M Na cacodylate buffer at 4°C. Samples were post-fixed with 1% osmium tetroxide/0.1 M Na cacodylate buffer, washed with buffer followed by MilliQ water, bloc stained with 3% aqueous uranyl acetate, dehydrated in ascending ethanol concentrations, rinsed briefly in propylene oxide, then embedded and polymerized in Taab epoxy resin. Ultrathin sections were cut and mounted on Pioloform-coated copper grids and stained with lead citrate. Immunogold labeling was carried out as described (McDonald et al., 1995) using rabbit polyclonal antibody to GFP (Abcam, ab6556) diluted 1:500 and goat-anti-rabbit IgG 10nm gold-conjugated (BB International) diluted 1:400. Samples were examined on a Jeol 1200EX Mark II transmission electron microscope and digital images recorded with a 1K 1.3M pixel High Sensitivity AMT Advantage ER-150 CCD camera system.

3. Results

3.1 Crystalloid formation occurs during the early part of ookinete development

We previously described parasite line *Pb*LAP3/GFP, which expresses *Pb*LAP3::GFP fusion protein that is efficiently targeted to the crystalloid (Saeed et al., 2010). This parasite line therefore provides a useful molecular marker for the crystalloid organelle, which we used here to study its formation during ookinete development. Ookinete cultures were set up from gametocytemic mouse blood and crystalloid formation was assessed at different times post-gametogenesis. The first clear signs of ookinete development were visible at 5h, with the spherical zygotes displaying a short protrusion corresponding to the apical end of the ookinete (Fig 1A). The distribution of GFP fluorescence at 5h was similar to earlier time points including female gametocytes, corresponding to a large and somewhat patchy extranuclear region (Fig. 1A). Consistent with this, immunogold EM of *Pb*LAP3/GFP gametocytes showed labelling of a large and seemingly discrete region of extranuclear cytoplasm (Fig. 1B). Although the relatively harsh fixation protocol required for optimal antibody-antigen binding poorly preserves the subcellular structures precluding a definitive allocation of the label, its distribution is consistent with that of the extensive ER present in female *P. berghei* gametocytes (Olivieri et al., 2015). In addition, LAP3::GFP co-localized with a red fluorescent ER marker in live cells (Fig. 1C). These combined observations indicate that LAP3 is present predominantly in the ER lumen in female gametocytes and during the early stages of ookinete development, which is in full agreement with the presence of a canonical ER signal peptide in *Pb*LAP3 and its orthologues (Claudianos et al., 2002; Pradel et al., 2004). At 6h the distribution of LAP3::GFP had become more punctate, possibly reflecting accumulation of the protein at ER exit sites (Fig. 1A). The first clear signs of crystalloid formation became apparent by 7h: retorts were now showing one or two evident, albeit weak fluorescent spots (Fig. 1A). By 10h crystalloid formation was all but complete, the cells now possessing two bright fluorescent spots within the spherical part of the retort, and four hours later the crystalloids had begun moving into

the 'ookinete' part of the retort (Fig. 1A). The crystalloids remained until ookinete development had completed, after which they were found located mostly, but not exclusively, at opposite sides of the nucleus (Fig. 1A). The large majority of mature ookinetes at 24h post-gametogenesis possessed two crystalloids (77%), with the remainder having either one (5%) or three (18%) crystalloids (n=100). The combined observations demonstrate that crystalloid formation takes place predominantly in the spherical 'zygote' part of the retort during the first 10h of ookinete development.

3.2 Crystalloids biogenesis involves transport and assembly of subunit vesicles

All LAP family members possess at least one LCCL domain, with the exception of LAP5. The latter is included in the family by virtue of being a close structural paralogue of LAP3, with an identical domain topology except for the (missing) LCCL domain (Dessens et al., 2011). The fact that *Pb*LAP5 is necessary for normal parasite development and sporozoite transmission in its own right (Ecker et al., 2008) suggested that the LCCL domain of *Pb*LAP3 could be nonessential for protein function. To test this hypothesis the LCCL domain was removed from *Pb*LAP3, thereby turning it into a *Pb*LAP5-like protein. To achieve this, the sequence corresponding to the LCCL domain was removed from the *pblap3::gfp* allele to generate parasite line *Pb*LAP3/LCCL-KO (Fig. 2A). This parasite expresses *Pb*LAP3 without its LCCL domain, but with a C-terminal GFP tag. Different clonal populations of this parasite line were obtained and validated by diagnostic PCR, which showed integration of the selectable marker gene into the *pblap3* locus, as well as the presence of the ~400bp deletion in the mutant *lap3::gfp* allele (Fig. 2B). Gametocytes of *Pb*LAP3/LCCL-KO parasites exhibited GFP fluorescence in gametocytes similar to *Pb*LAP3/GFP parasites, and readily developed into ookinetes in culture. Western blot with anti-GFP antibody detected a GFP fusion protein in *Pb*LAP3/LCCL-KO parasites that was ~15kDa smaller than the equivalent LAP3::GFP fusion protein detected in *Pb*LAP3/GFP parasites, consistent with deletion of the LCCL domain (Fig. 2C). In addition, an approximately 27kDa protein likely corresponding to cleaved GFP was present in the *Pb*LAP3/LCCL-KO parasite line. The enhanced cleavage of GFP in

242 this parasite compared to *Pb*LAP3/GFP could reflect an altered conformation of the LAP complex
243 in response to the LCCL deletion of *Pb*LAP3.
244 Cultured ookinetes examined by confocal microscopy at 24h post-gametogenesis displayed
245 no apparent differences between *Pb*LAP3/LCCL-KO and *Pb*LAP3/GFP control parasite lines, the
246 majority of ookinetes displaying two fluorescent spots characteristic of the crystalloids (Fig. 3A).
247 Indeed, both parasite lines had comparable infectivity in mosquitoes (58±22 oocysts per mosquito
248 for *Pb*LAP3/GFP; 35±9 for *Pb*LAP3/LCCL-KO, n=20; p=0.98, Mann-Whitney test) and formed
249 sporozoites that were readily transmitted by mosquito bite. These results demonstrate that *Pb*LAP3
250 without its LCCL domain retains biological activity. In contrast, when *Pb*LAP3/LCCL-KO
251 ookinetes were examined at 18h post-gametogenesis they looked markedly different from
252 *Pb*LAP3/GFP control ookinetes, possessing notably more and generally smaller fluorescent spots
253 (Fig. 3A). The same was observed in different clones of the LCCL domain deletion mutant,
254 indicating this phenotype was not the result of clonal variation. TEM examination of these
255 ookinetes revealed the presence of more and much smaller clusters of subunit vesicles (Fig. 3B).
256 Assessing the number of fluorescent spots/crystalloids in a time course showed a gradual decrease
257 in their number (Fig. 4A), indicating that the mini-crystalloids congregate during crystalloid
258 formation. On many occasions we observed *Pb*LAP3/LCCL-KO ookinetes with several smaller
259 crystalloids in close proximity of each other, seemingly in the process of merging (Fig. 4B). A
260 similar process was observed by TEM (Fig. 4C). Interestingly, in control LAP3/GFP ookinetes
261 there was also a significant, albeit small, decrease in the mean number of crystalloids per cell
262 between 18h and 24h post-gametogenesis (Fig. 4A), indicating that in wildtype ookinetes, too,
263 crystalloids form by an assembly process. Indeed, when we examined young oocysts on the basal
264 side of *Anopheles stephensi* midguts at 2 days post-infection, the large majority (96%, n=50)
265 possessed only a single large crystalloid (Fig. 4D), with the remaining oocysts possessing two
266 closely apposed crystalloids. Thus, crystalloid assembly continues up to development of young
267 oocysts.

3.3 Crystalloid assembly requires microtubule-based vesicle transport

The apparent transport and assembly of crystalloid subunits suggested that crystalloid formation requires vesicle transport. There is extensive evidence that transport of membrane vesicles in eukaryotic cells takes place along tracks of cytoskeletal polymers (Goodson et al., 1997). To investigate this hypothesis, we tested the effects of chemical inhibitors of cytoskeleton-based cargo transport. In a first set of experiments, inhibitors were added to *Pb*LAP3/LCCL-KO ookinete cultures at 18h and the effects on crystalloid assembly were assessed at 24h. Paclitaxel, which interferes with microtubule dynamics and impedes microtubule-based cargo transport *in vivo* (Hamm-Alvarez et al., 1994; Sonee et al., 1998; Schnaeker et al., 2004; Hellal et al., 2011) had a marked effect on crystalloid formation in a dose-dependent manner, compared to the DMSO solvent control that did not affect crystalloid assembly (Fig. 5A). Paclitaxel at 1µ*M* effectively stopped progression of crystalloid assembly, resulting in ookinetes with more and smaller spots similar to the 18h starting point. To a lesser extent, cytochalasin D, which interferes with actin filament formation and impedes actin/myosin-based cargo transport, significantly inhibited this process (Fig. 5A). In contrast, there was no discernible effect of either of the inhibitors on crystalloid formation in control *Pb*LAP3/GFP ookinetes (Fig. 5B). This was as expected, because assembled crystalloids are already present at 18h when the inhibitors were added (Fig. 3A). These observations indicate that crystalloid biogenesis requires both microtubule- and actin filament-dependent cargo transport.

To test the effects of cargo transport inhibitors on crystalloid formation in wildtype parasites, 1µ*M* paclitaxel was added at 6h post-gametogenesis to *Pb*LAP3/GFP ookinete cultures. This is the earliest time this compound can be added without preventing development of mature ookinetes (Kumar et al., 1985). At 24h post-gametogenesis, paclitaxel-treated *Pb*LAP3/GFP ookinetes possessed significantly more and smaller spots (Fig. 6A) than the DMSO-treated controls (paclitaxel: 2-8 spots, mean of 4.5; DMSO: 1-3 spots, mean of 1.6; n=20; $p<0.01$, Mann-Whitney

294 test). Control and paclitaxel-treated ookinetes had comparable viability levels at 24h post-
295 gametogenesis (DMSO 98% viability; paclitaxel 97% viability; n=100), indicating that the increase
296 in the number of fluorescent spots was not the result of cytotoxicity of the inhibitor to the parasite.
297 Moreover, TEM examination of paclitaxel-treated LAP3/GFP ookinetes showed an overall normal
298 development of subcellular organelles and structures, including the subpellicular microtubules (Fig.
299 6). Interestingly, bundels of microtubules were observed in close proximity to crystalloids
300 /crystalloid assembly sites (Fig. 6). Similar structures were not found in untreated ookinetes. These
301 results combined indicate that crystalloid formation involves microtubules. The fact we can
302 replicate, at least in part, the *Pb*LAP3/LCCL-KO phenotype in *Pb*LAP3/GFP parasites by adding
303 cargo transport inhibitors suggests that the basic processes of crystalloid biogenesis are the same
304 between the wildtype and mutant parasites. Accordingly, the *Pb*LAP3/LCCL-KO mutant parasite
305 appears to exhibit attenuated crystalloid genesis manifested in a delay in crystalloid assembly.
306 Despite this delay, normal crystalloids are present by the time of ookinete-to-oocyst transition (Fig.
307 3A).
308
309 *3.4 Knockout of PbLAP3 abolishes crystalloid biogenesis*
310 To determine if the delayed crystalloid biogenesis observed in the *Pb*LAP3/LCCL-KO parasites
311 was a complete or partial loss-of-function phenotype, we generated a *Pb*LAP3 null mutant parasite
312 line named *Pb*LAP3-KO using double crossover homologous recombination (Fig. 7A). Correct
313 integration of the selectable marker into the target locus was confirmed by Southern analysis of
314 *Hin*dIII-digested genomic DNA (Fig. 7B): a *pblap3*-specific probe detected bands of 3.4kb and
315 9.5kb in wildtype and *Pb*LAP3/GFP parasites, respectively, but no signal in *Pb*LAP3-KO parasites,
316 as expected (Figs. 7A, B). Conversely, a *hdhfr*-specific probe detected bands of 7.1kb and 9.5kb in
317 *Pb*LAP3-KO and *Pb*LAP3/GFP parasites, respectively, but no signal in wildtype parasites, as
318 predicted (Figs. 7A, B). *Pb*LAP3-KO parasites displayed normal blood stage development,
319 produced gametocytes and readily formed oocysts in *Anopheles stephensi* vector mosquitoes

(58±22 oocysts per mosquito for *Pb*LAP3/GFP; 56±26 for *Pb*LAP3-KO, n=20). However, the large majority of oocysts (~98%) failed to produce sporozoites (Fig. 7C). In line with this observation, we were repeatedly unable to transmit this parasite by mosquito bite. The same phenotype was observed with a different clone of the *Pb*LAP3-KO line. By contrast, *Pb*LAP3/GFP control parasites exhibited normal sporulation (Fig. 7C) and were readily transmitted. These observations demonstrate that *Pb*LAP3 is necessary for the production of infective sporozoites in mosquitoes.

When we examined *Pb*LAP3-KO ookinetes by TEM we could not find any evidence for crystalloid biogenesis, while other known ookinete structures and organelles were normally present (Fig. 7D). Thin sections of control *Pb*LAP3/GFP ookinetes had crystalloids in 83% of distinct cells examined (n=82), while none were found in equivalent sections of *Pb*LAP3-KO ookinetes (n=71), demonstrating that *Pb*LAP3 is essential for crystalloid biogenesis ($p<0.0001$, Fisher's exact test). This observation strongly points to a functional link between crystalloid formation in the ookinete, and sporogenesis in the oocyst. The *Pb*LAP3-KO phenotype clearly is more severe than that of the *Pb*LAP3/LCCL-KO mutant, confirming that the latter is indeed an intermediate phenotype.

335

336 **4. Discussion**

337 This study shows for the first time is that crystalloid biogenesis in the rodent malaria parasite
338 species *P. berghei* is achieved via a process of sequential subunit vesicle formation, transport and
339 coordinated assembly (Fig. 8), and that these processes are microtubule-dependent. These processes
340 are likely to be conserved in human malaria parasite species such as *P. falciparum,* which possesses
341 crystalloids virtually indistinguishable from those found in *P. berghei* (Meis and Ponnudurai, 1987).
342 Our data show furthermore that crystalloid formation happens to a large extent during the early
343 stages of ookinete development (Fig. 1A), but does not complete until oocyst transition ultimately
344 giving rise to a single crystalloid organelle in the oocyst (Fig. 4D).

345 The demonstrated localisation of the LAPs in the crystalloid (Carter et al., 2008; Saeed et al.,
346 2010, 2013) suggests that the LAP complex is part of the cargo of its subunit vesicles. Interactions
347 of major cargo molecules with the COPII machinery contribute to the formation of vesicles budding
348 from the ER (Aridor et al., 1999). This could explain why deletion or alteration of *Pb*LAP3
349 adversely affects crystalloid formation, as such interactions could be compromised. In the *Pb*LAP3
350 null mutant we found no evidence of crystalloid assembly, indicating that the subunit vesicles are
351 not formed in the first place. The LAPs are co-dependent for conformation and stability (Pradel et
352 al., 2006; Simon et al., 2009; Saeed et al., 2012), and it is therefore probable that in the *Pb*LAP3
353 null mutant a functional LAP complex is unable to form in the ER lumen (step 2 in Fig. 8), which in
354 turn could prevent formation of crystalloid subunit vesicles at their ER exit sites. This notion is
355 further supported by observations that dysfunctional *Pb*LAP1 lacking its two tandem scavenger
356 receptor cysteine-rich (SRCR) domains remains in the ER (Carter et al., 2008). By contrast, in the
357 *Pb*LAP3/LCCL-KO mutant, subunit vesicles are clearly formed and engage with the intrinsic
358 mechanisms of vesicle transport allowing crystalloid assembly to proceed and produce normal
359 crystalloids by the time of oocyst transition. In this mutant, subunit vesicle formation could be

slowed down as a result of a suboptimal interaction of the altered LAP complex with the vesicle budding machinery (step 3 in Fig. 8).

Our observation that crystalloid biogenesis is sensitive to inhibitors of both microtubule- and actin filament-based transport (Fig. 4A) implies that a degree of filament switching takes place (Langford, 1995; Schroeder et al., 2010). The classic dual filament model of cargo transport uses microtubules for 'long distance' and actin filaments for local dynamic interactions (Schroeder et al., 2010). The same may be true for crystalloid formation, as the effect of cytochalasin D on vesicle assembly is much less pronounced than that of paclitaxel (Fig. 4A). Moreover, cytochalasin D added at 1μ*M* to *Pb*LAP3/LCCL-KO ookinete cultures at 6h post-gametogenesis did not significantly increase the adverse effect on crystalloid assembly (1-5 spots, mean of 3.0) compared to its addition at 18h (2-5 spots, mean of 3.3), despite having more time to interfere with the process. These observation suggest that the actin filament-based transport could indeed be acting downstream of microtubule-dependent transport.

Our data using LAP3/GFP parasites show that crystalloids form early in ookinete development, within the spherical part of the retort (Fig. 1A). Because this part of the cell does not possess a pellicle or subpellicular microtubules, these unusually stable cortical microtubules (Cyrklaff et al., 2007) are unlikely to be involved in crystalloid biogenesis. In many regions of the cytoplasm microtubules are much more dynamic polymers that undergo continual assembly and disassembly (Waterman-Storer and Salmon, 1997; Jordan and Wilson, 2004), and our observations suggest that an alternative and more dynamic microtubule system could be involved in crystalloid assembly. In the large majority of cells crystalloid formation initially produces two ‘sub’crystalloids (Figs. 1A and 5A), which persist in most ookinetes until oocyst transition when they merge into a single crystalloid (Fig. 4D). This suggests that the vesicle assembly process that gives rise to crystalloid formation is not random, but uses specific ‘assembly sites’. Given the tubulin-dependence of crystalloid biogenesis, it is attractive to speculate that these assembly sites are orchestrated by microtubule organising centres (MTOCs), allowing subunit vesicles to move toward

386 them along microtubules using dynein motors. This hypothesis is supported by our observation of
387 microtubules in close proximity to crystalloids in paclitaxel-treated ookinetes (Fig. 6). Potential
388 MTOCs in the zygote could include the spindle pole plaques (Sinden et al., 1985), cytoplasmic
389 centrioles (Aikawa et al., 1984), or Golgi membranes that can nucleate microtubules (Miller et al.,
390 2009; Zhu and Kaverina, 2013).

391 In the context of LAP family members forming a functional protein complex, it is not
392 surprising that knockout of *Pb*LAP3 results in loss of sporozoite development and transmission, as
393 is the case for its family members (Claudianos et al., 2002; Raine et al., 2007; Carter et al., 2008;
394 Ecker et al., 2008; Lavazec et al., 2009). The fact that crystalloids are absent in the *Pb*LAP3 null
395 mutant (Fig 7D) shows that the *Pb*LAP3/LCCL-KO mutant exhibits a partial loss-of-function
396 phenotype. Absence of crystalloid formation was also observed in *Pb*LAP1 (*Pb*SR) null mutants
397 (Carter et al., 2008), and the lack of crystalloid formation reported here for *Pb*LAP3 thus makes it
398 likely that this phenomenon is a shared feature of all LAP null mutants in *P. berghei*. The dramatic
399 defect in sporozoite development in *Pb*LAP null mutants is thus consistent with absence of
400 crystalloid biogenesis, in turn suggesting that these organelles, or the cargo carried by them, are
401 required for normal oocyst maturation and ensuing sporozoite transmission. Preventing crystalloid
402 formation could therefore present an attractive strategy to block malaria transmission. One way to
403 achieve this could be by chemically interfering with the formation of a functional LAP complex,
404 effectively replicating the LAP null mutant phenotype. The gametocyte-specific expression of many
405 LAPs (Pradel et al., 2006; Carter et al., 2008; Scholz et al., 2008; Simon et al., 2009; Saeed et al.,
406 2010, 2013) means that LAP complex formation could be targeted in the human host, before the
407 parasite enters the mosquito vector. As such, this transmission-blocking approach would not be
408 reliant on the uptake of the inhibitor with the blood meal of the mosquito, which is required in
409 transmission-blocking strategies that target development or progression of the life stages within the
410 midgut lumen of the mosquito (*i.e.* gametes, zygotes and ookinetes). The 'delayed death' aspect of
411 targeting LAP complex formation, and hence crystalloid biogenesis, would also benefit this strategy

as the ookinete and oocyst loads in the mosquito are not reduced. The potential risk of increasing fitness of the insect by lowering its parasite burden is one of the caveats of current transmission-blocking strategies being developed (Dawes et al., 2009; Churcher et al., 2011), as reductions in sporozoite load could be counteracted by the mosquitoes being infective for longer, increasing their vectorial capacity. We therefore propose that transmission blockade through targeting the crystalloid organelle could provide a valuable new approach to complement the existing arsenal of malaria transmission control strategies being employed or developed.

The discoveries made here regarding LAP function and crystalloid formation are also relevant in the context of other apicomplexan parasites. Biogenesis of crystalloids by active vesicle assembly could be a specific adaptation of the genus *Plasmodium*, since many other genera (including the medically and veterinary important *Toxoplasma, Eimeria, Babesia* and *Theileria*) do not possess crystalloids, but do encode LAP orthologues. A conserved function of apicomplexan LAPs in vesicle, rather than crystalloid, formation would allow for a role that could potentially serve the broad spectrum of life cycles present among members of this large and important phylum.

Acknowledgements

This work was supported by the Wellcome Trust, grants 076648 and 088449. We thank E McCarthy and M McCrossan for assistance with microscopy.

References

Aikawa, M., Carter, R., Ito, Y., Nijhout, M.M., 1984. New observations on gametogenesis, fertilization, and zygote transformation in *Plasmodium gallinaceum*. J Protozool 31, 403-413.

Al-Khattaf, F.S., Tremp, A.Z., Dessens, J.T., 2015. *Plasmodium* alveolins possess distinct but structurally and functionally related multi-repeat domains. Parasitol Res 114, 631-639.

Arai, M., Billker, O., Morris, H.R., Panico, M., Delcroix, M., Dixon, D., Ley, S.V., Sinden, R.E., 2001. Both mosquito-derived xanthurenic acid and a host blood-derived factor regulate gametogenesis of *Plasmodium* in the midgut of the mosquito. Mol Biochem Parasitol 116, 17-24.

Aridor, M., Bannykh, S.I., Rowe, T., Balch, W.E., 1999. Cargo can modulate COPII vesicle formation from the endoplasmic reticulum. J Biol Chem 274, 4389-4399.

Carter, V., Shimizu, S., Arai, M., Dessens, J.T., 2008. PbSR is synthesized in macrogametocytes and involved in formation of the malaria crystalloids. Mol Microbiol 68, 1560-1569.

Churcher, T.S., Dawes, E.J., Sinden, R.E., Christophides, G.K., Koella, J.C., Basanez, M.G., 2011. Population biology of malaria within the mosquito: density-dependent processes and potential implications for transmission-blocking interventions. Malar J 9, 311.

Claudianos, C., Dessens, J.T., Trueman, H.E., Arai, M., Mendoza, J., Butcher, G.A., Crompton, T., Sinden, R.E., 2002. A malaria scavenger receptor-like protein essential for parasite development. Mol Microbiol 45, 1473-1484.

Cyrklaff, M., Kudryashev, M., Leis, A., Leonard, K., Baumeister, W., Menard, R., Meissner, M., Frischknecht, F., 2007. Cryoelectron tomography reveals periodic material at the inner side of subpellicular microtubules in apicomplexan parasites. J Exp Med 204, 1281-1287.

Dawes, E.J., Churcher, T.S., Zhuang, S., Sinden, R.E., Basanez, M.G., 2009. *Anopheles* mortality is both age- and *Plasmodium*-density dependent: implications for malaria transmission. Malar J 8, 228.

Delrieu, I., Waller, C.C., Mota, M.M., Grainger, M., Langhorne, J., Holder, A.A., 2002. PSLAP, a protein with multiple adhesive motifs, is expressed in *Plasmodium falciparum* gametocytes. Mol Biochem Parasitol 121, 11-20.

Dessens, J.T., Beetsma, A.L., Dimopoulos, G., Wengelnik, K., Crisanti, A., Kafatos, F.C., Sinden, R.E., 1999. CTRP is essential for mosquito infection by malaria ookinetes. EMBO J 18, 6221-6227.

Dessens, J.T., Sinden, R.E., Claudianos, C., 2004. LCCL proteins of apicomplexan parasites. Trends Parasitol 20, 102-108.

Dessens, J.T., Saeed, S., Tremp, A.Z., Carter, V., 2011. Malaria crystalloids: specialized structures for parasite transmission? Trends Parasitol 27, 106-110.

Ecker, A., Bushell, E.S., Tewari, R., Sinden, R.E., 2008. Reverse genetics screen identifies six proteins important for malaria development in the mosquito. Mol Microbiol 70, 209-220.

Garnham, P.C., Bird, R.G., Baker, J.R., 1962. Electron microscope studies of motile stages of malaria parasites. III. The ookinetes of *Haemamoeba* and *Plasmodium*. Trans R Soc Trop Med Hyg 56, 116-120.

Garnham, P.C., Bird, R.G., Baker, J.R., Desser, S.S., el-Nahal, H.M., 1969. Electron microscope studies on motile stages of malaria parasites. VI. The ookinete of *Plasmodium berghei yoelii* and its transformation into the early oocyst. Trans R Soc Trop Med Hyg 63, 187-194.

Goodson, H.V., Valetti, C., Kreis, T.E., 1997. Motors and membrane traffic. Curr Opin Cell Biol 9, 18-28.

Hamm-Alvarez, S.F., Alayof, B.E., Himmel, H.M., Kim, P.Y., Crews, A.L., Strauss, H.C., Sheetz, M.P., 1994. Coordinate depression of bradykinin receptor recycling and microtubule-dependent transport by taxol. Proc Natl Acad Sci U S A 91, 7812-7816.

Hellal, F., Hurtado, A., Ruschel, J., Flynn, K.C., Laskowski, C.J., Umlauf, M., Kapitein, L.C., Strikis, D., Lemmon, V., Bixby, J., Hoogenraad, C.C., Bradke, F., 2011. Microtubule stabilization reduces scarring and causes axon regeneration after spinal cord injury. Science 331, 928-931.

Janse, C.J., van der Klooster, P.F., van der Kaay, H.J., van der Ploeg, M., Overdulve, J.P., 1986. DNA synthesis in *Plasmodium berghei* during asexual and sexual development. Mol Biochem Parasitol 20, 173-182.

Janse, C.J., Ramesar, J., Waters, A.P., 2006. High-efficiency transfection and drug selection of genetically transformed blood stages of the rodent malaria parasite *Plasmodium berghei*. Nat Protoc 1, 346-356.

Jordan, M.A., Wilson, L., 2004. Microtubules as a target for anticancer drugs. Nat Rev Cancer 4, 253-265.

Khater, E.I., Sinden, R.E., Dessens, J.T., 2004. A malaria membrane skeletal protein is essential for normal morphogenesis, motility, and infectivity of sporozoites. J Cell Biol 167, 425-432.

Kumar, N., Aikawa, M., Grotendorst, C., 1985. *Plasmodium gallinaceum*: critical role for microtubules in the transformation of zygotes into Ookinetes. Exp Parasitol 59, 239-247.

Langford, G.M., 1995. Actin- and microtubule-dependent organelle motors: interrelationships between the two motility systems. Curr Opin Cell Biol 7, 82-88.

Lavazec, C., Moreira, C.K., Mair, G.R., Waters, A.P., Janse, C.J., Templeton, T.J., 2009. Analysis of mutant *Plasmodium berghei* parasites lacking expression of multiple PbCCp genes. Mol Biochem Parasitol 163, 1-7.

Mann, T., Beckers, C., 2001. Characterization of the subpellicular network, a filamentous membrane skeletal component in the parasite *Toxoplasma gondii*. Mol Biochem Parasitol 115, 257-268.

McDonald, V., McCrossan, M.V., Petry, F., 1995. Localization of parasite antigens in *Cryptosporidium parvum*-infected epithelial cells using monoclonal antibodies. Parasitology 110 (Pt 3), 259-268.

Meis, J.F., Ponnudurai, T., 1987. Ultrastructural studies on the interaction of *Plasmodium falciparum* ookinetes with the midgut epithelium of *Anopheles stephensi* mosquitoes. Parasitol Res 73, 500-506.

Miller, P.M., Folkmann, A.W., Maia, A.R., Efimova, N., Efimov, A., Kaverina, I., 2009. Golgi-derived CLASP-dependent microtubules control Golgi organization and polarized trafficking in motile cells. Nat Cell Biol 11, 1069-1080.

Morrissette, N.S., Sibley, L.D., 2002. Cytoskeleton of apicomplexan parasites. Microbiol Mol Biol Rev 66, 21-38.

Olivieri, A., Bertuccini, L., Deligianni, E., Franke-Fayard, B., Curra, C., Siden-Kiamos, I., Hanssen, E., Grasso, F., Superti, F., Pace, T., Fratini, F., Janse, C.J., Ponzi, M., 2015. Distinct properties of the egress-related osmiophilic bodies in male and female gametocytes of the rodent malaria parasite *Plasmodium berghei*. CelL Microbiol.

Pradel, G., Hayton, K., Aravind, L., Iyer, L.M., Abrahamsen, M.S., Bonawitz, A., Mejia, C., Templeton, T.J., 2004. A multidomain adhesion protein family expressed in *Plasmodium falciparum* is essential for transmission to the mosquito. J Exp Med 199, 1533-1544.

Pradel, G., Wagner, C., Mejia, C., Templeton, T.J., 2006. *Plasmodium falciparum*: Co-dependent expression and co-localization of the PfCCp multi-adhesion domain proteins. Exp Parasitol 112, 263-268.

Raine, J.D., Ecker, A., Mendoza, J., Tewari, R., Stanway, R.R., Sinden, R.E., 2007. Female inheritance of malarial lap genes is essential for mosquito transmission. PLoS Pathog 3, e30.

Saeed, S., Carter, V., Tremp, A.Z., Dessens, J.T., 2010. *Plasmodium berghei* crystalloids contain multiple LCCL proteins. Mol Biochem Parasitol 170, 49-53.

Saeed, S., Tremp, A.Z., Dessens, J.T., 2012. Conformational co-dependence between *Plasmodium berghei* LCCL proteins promotes complex formation and stability. Mol Biochem Parasitol 185, 170-173.

533 Saeed, S., Carter, V., Tremp, A.Z., Dessens, J.T., 2013. Translational repression controls temporal
534 expression of the *Plasmodium berghei* LCCL protein complex. Mol Biochem Parasitol 189,
535 38-42.
536 Schnaeker, E.M., Ossig, R., Ludwig, T., Dreier, R., Oberleithner, H., Wilhelmi, M., Schneider,
537 S.W., 2004. Microtubule-dependent matrix metalloproteinase-2/matrix metalloproteinase-9
538 exocytosis: prerequisite in human melanoma cell invasion. Cancer Res 64, 8924-8931.
539 Scholz, S.M., Simon, N., Lavazec, C., Dude, M.A., Templeton, T.J., Pradel, G., 2008. PfCCp
540 proteins of *Plasmodium falciparum*: gametocyte-specific expression and role in
541 complement-mediated inhibition of exflagellation. Int J Parasitol 38, 327-340.
542 Schroeder, H.W., 3rd, Mitchell, C., Shuman, H., Holzbaur, E.L., Goldman, Y.E., 2010. Motor
543 number controls cargo switching at actin-microtubule intersections *in vitro*. Curr Biol 20,
544 687-696.
545 Simon, N., Scholz, S.M., Moreira, C.K., Templeton, T.J., Kuehn, A., Dude, M.A., Pradel, G., 2009.
546 Sexual stage adhesion proteins form multi-protein complexes in the malaria parasite
547 *Plasmodium falciparum*. J Biol Chem 284, 14537-14546.
548 Sinden, R.E., Hartley, R.H., Winger, L., 1985. The development of *Plasmodium* ookinetes in vitro:
549 an ultrastructural study including a description of meiotic division. Parasitology 91 (Pt 2),
550 227-244.
551 Sonee, M., Barron, E., Yarber, F.A., Hamm-Alvarez, S.F., 1998. Taxol inhibits endosomal-
552 lysosomal membrane trafficking at two distinct steps in CV-1 cells. Am J Physiol 275,
553 C1630-1639.
554 Terzakis, J.A., Vanderberg, J.P., Weiss, M.M., 1976. Viruslike particles in malaria parasites. J
555 Parasitol 62, 366-371.
556 Trefiak, W.D., Desser, S.S., 1973. Crystalloid inclusions in species of *Leucocytozoon*,
557 *Parahaemoproteus*, and *Plasmodium*. J Protozool 20, 73-80.
558 Tremp, A.Z., Carter, V., Saeed, S., Dessens, J.T., 2013. Morphogenesis of *Plasmodium* zoites is
559 uncoupled from tensile strength. Mol Microbiol 89, 552-564.
560 Trexler, M., Banyai, L., Patthy, L., 2000. The LCCL module. Eur J Biochem 267, 5751-5757.
561 Trueman, H.E., Raine, J.D., Florens, L., Dessens, J.T., Mendoza, J., Johnson, J., Waller, C.C.,
562 Delrieu, I., Holders, A.A., Langhorne, J., Carucci, D.J., Yates, J.R., 3rd, Sinden, R.E., 2004.
563 Functional characterization of an LCCL-lectin domain containing protein family in
564 *Plasmodium berghei*. J Parasitol 90, 1062-1071.
565 Waterman-Storer, C.M., Salmon, E.D., 1997. Microtubule dynamics: treadmilling comes around
566 again. Curr Biol 7, R369-372.
567 Zhu, X., Kaverina, I., 2013. Golgi as an MTOC: making microtubules for its own good. Histochem
568 Cell Biol 140, 361-367.
569

Figure Legends

570

571 **Fig. 1** Crystalloid formation during ookinete development. **A**: Confocal microscope images
572 showing typical subcellular distribution of LAP3::GFP at different time points after gametogenesis.
573 White arrows at 7h mark early crystalloids. **B**: Representative immuno electron micrograph of a
574 LAP3/GFP gametocyte section labelled with anti-GFP primary antibodies and gold-conjugated
575 secondary antibodies. The presence of gold particles (marked by arrows) is limited to a large
576 extranuclear region of cytoplasm (encircled). Also marked are the nucleus (N) and hemozoin-
577 containing vacuoles (*). **C**: Confocal microscope image of a zygote of parasite line *Pb*LAP3/GFP at
578 5h post-gametogenesis, co-stained with the ER marker ER-ID Red. Blue DNA stain (Hoechst) stain
579 labels the nucleus in the overlay image.

580

581 **Fig. 2** Molecular analyses of *Pb*LAP3/LCCL-KO parasites **A**: Schematic diagram of the *pblap3*
582 allele structure in parasite lines *Pb*LAP3/GFP and *Pb*LAP3/LCCL-KO. Indicated are the primer
583 sites (P1-P4) used for diagnostic PCR. The LCCL domain is denoted with a black box. **B**:
584 Diagnostic PCR with primers P1 (ACAAAGAATTCATGGTTGGTTCGCTAAACT) and P2
585 (CCTCAAGATAGTTACGAATTTAAC) for integration of the *hdhfr* selectable marker gene into
586 the *pblap3* locus (top panel), and with primers P3
587 (ACGAAGTTATCAGTCGAGGTACCTAGCGGAAACAACAATGTTC) and P4
588 (ATGAGGGCCCCTAAGCTATTTTTAATAATTTGTATCGAAAGTATAGTTG) for
589 absence/presence of the LCCL domain deletion (bottom panel). **C**: Western blot of gametocytes
590 using anti-GFP antibodies. The blot shows bands corresponding to the full-length (~150kDa) and
591 LCCL domain-lacking (~135kDa) *Pb*LAP3::GFP fusion proteins, cleaved GFP (~27kDa), and a
592 ~65kDa host cell protein (*) that cross-reacts with the antibody (Saeed et al., 2012; Tremp et al.,
593 2013). Molecular weight markers are indicated on the left hand side.

594

595 **Fig. 3** Phenotypic analyses of *Pb*LAP3/LCCL-KO ookinetes. **A**: Confocal microscope images of
596 cultured *Pb*LAP3/LCCL-KO ookinetes at 18 h and 24 h post-gametogenesis, compared with
597 *Pb*LAP3/GFP control ookinetes. **B**: TEM images of *Pb*LAP3/GFP and *Pb*LAP3/LCCL-KO
598 ookinetes at 18 h post-gametogenesis. Crystalloids are encircled.
599
600 **Fig. 4** Crystalloids form via an assembly process. **A**: Time course of the number of fluorescent
601 spots/crystalloids per cell in cultured *Pb*LAP3/LCCL-KO ookinetes (open circles) at 18h, 21h and
602 24h post-gametogenesis, compared with *Pb*LAP3/GFP ookinetes (closed circles). Horizontal lines
603 denote mean values. Asterixs indicate statistically significant differences: $p<0.001$ (**) and
604 $p<0.0001$ (***) (Mann-Whitney). **B**: Confocal image and **C**: TEM image of 'merging' crystalloids
605 in *Pb*LAP3/LCCL-KO ookinetes. Crystalloids are encircled. **D**: Confocal image of a spherical
606 young oocyst located on an *Anopheles stephensi* midgut, typically possessing a single large
607 crystalloid.
608
609 **Fig. 5** Inhibitors of vesicle transport affect crystalloid biogenesis **A**: Scatter plot of the number of
610 fluorescent spots per cell in cultured *Pb*LAP3/LCCL-KO ookinetes and **B**: *Pb*LAP3/GFP ookinetes
611 at 24 h post-gametogenesis in the presence of paclitaxel or cytochalasin D and compared with
612 dimethyl sulfoxide (DMSO) solvent controls. Inhibitors were added at 18h post-gametogenesis.
613 Horizontal lines denote mean values. Asterixs indicate statistically significant differences: $p<0.05$
614 (*), $p<0.001$ (**) and $p<0.0001$ (***) (Mann-Whitney). **C**: Confocal image of a *Pb*LAP3/GFP
615 ookinete at 24h post-gametogenesis with 1 μ*M* paclitaxel added at 6h post-gametogenesis, showing
616 multiple crystalloids.
617
618 **Fig. 6** Association of microtubules and crystalloids. TEM images of thin sections of paclitaxel-
619 treated ookinetes. **A**: Transverse section through a bundle of microtubules (encircled white)
620 adjacent to a crystalloid (encircled black). White arrowheads mark subpellicular microtubules in

neighbouring ookinete. Black box marks pellicle membranes. **B**: Slightly more longitudinal cross-section through a bundle of microtubules (encircled white) within a crystalloid assembly site (crystalloids encircled black). **C**: Microtubules (white arrows) embedded within a crystalloid.

Fig. 7 Genotypic and phenotypic analyses of *Pb*LAP3 null mutant parasites. **A**: Schematic diagram of the *pblap3* allele structure in parental wildtype and transgenic *Pb*LAP3/GFP and *Pb*LAP3-KO parasite lines. Indicated are the *Hin*dIII restriction sites (H), sizes of the predicted *Hin*dIII restriction fragments, and regions used as probes (thick black lines). **B**: Southern blot analysis of HindIII-digested genomic DNA. Indicated are the sizes of bands in kb. **C**: Confocal images of a typical sporulating (*Pb*LAP3/GFP) and non-sporulating (*Pb*LAP3-KO) oocyst at 2 weeks post-infection. Hoechst DNA stain (blue) labels the nuclei. **D**: Transmission electron micrographs of mature ookinete sections typical of *Pb*LAP3/GFP and *Pb*LAP3-KO parasite lines. The crystalloid is marked with a black arrow. Also indicated are the nucleus (N) and apical complex (AC).

Fig. 8 Proposed model of crystalloid biogenesis in *P. berghei*. A single cell is depicted, which represents the transformation from gametocyte (left hand side), via the zygote and ookinete, to oocyst (right hand side). N = nucleus; ER = endoplasmic reticulum; CR = crystalloid. Key steps are indicated by numbers. Step 1: Translation of the LAPs in rough ER and translocation into ER lumen; Step 2: Assembly of the LAP family members into a functional protein complex; Step 3: Formation of the subunit vesicles at ER exit sites; Step 4: Transport of the subunit vesicles to (typically two) assembly sites; Step 5: Final merging of sub-crystalloids into a single organelle in the oocyst.

Figure 1

Click here to download high resolution image

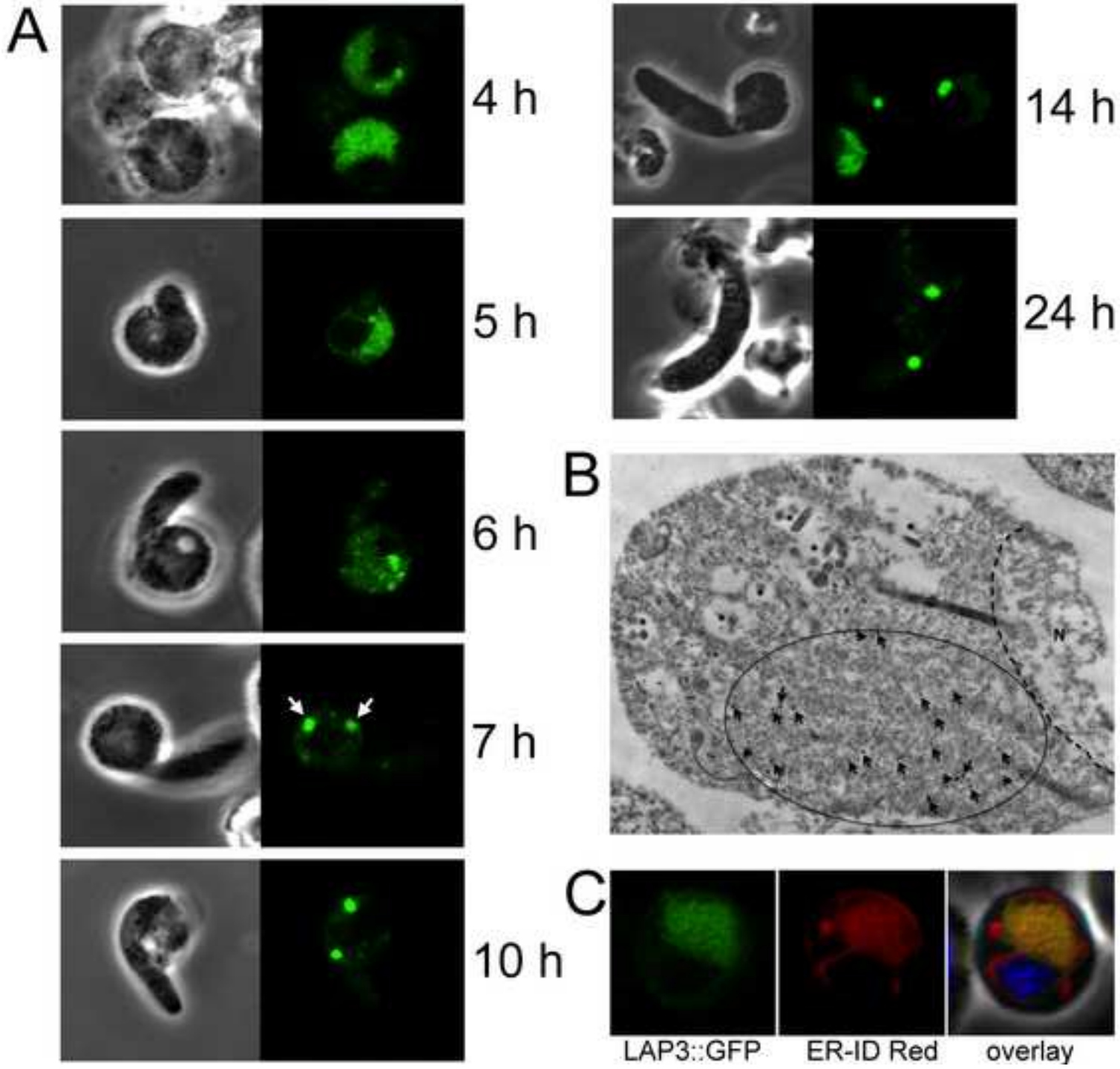

Figure 2

Click here to download high resolution image

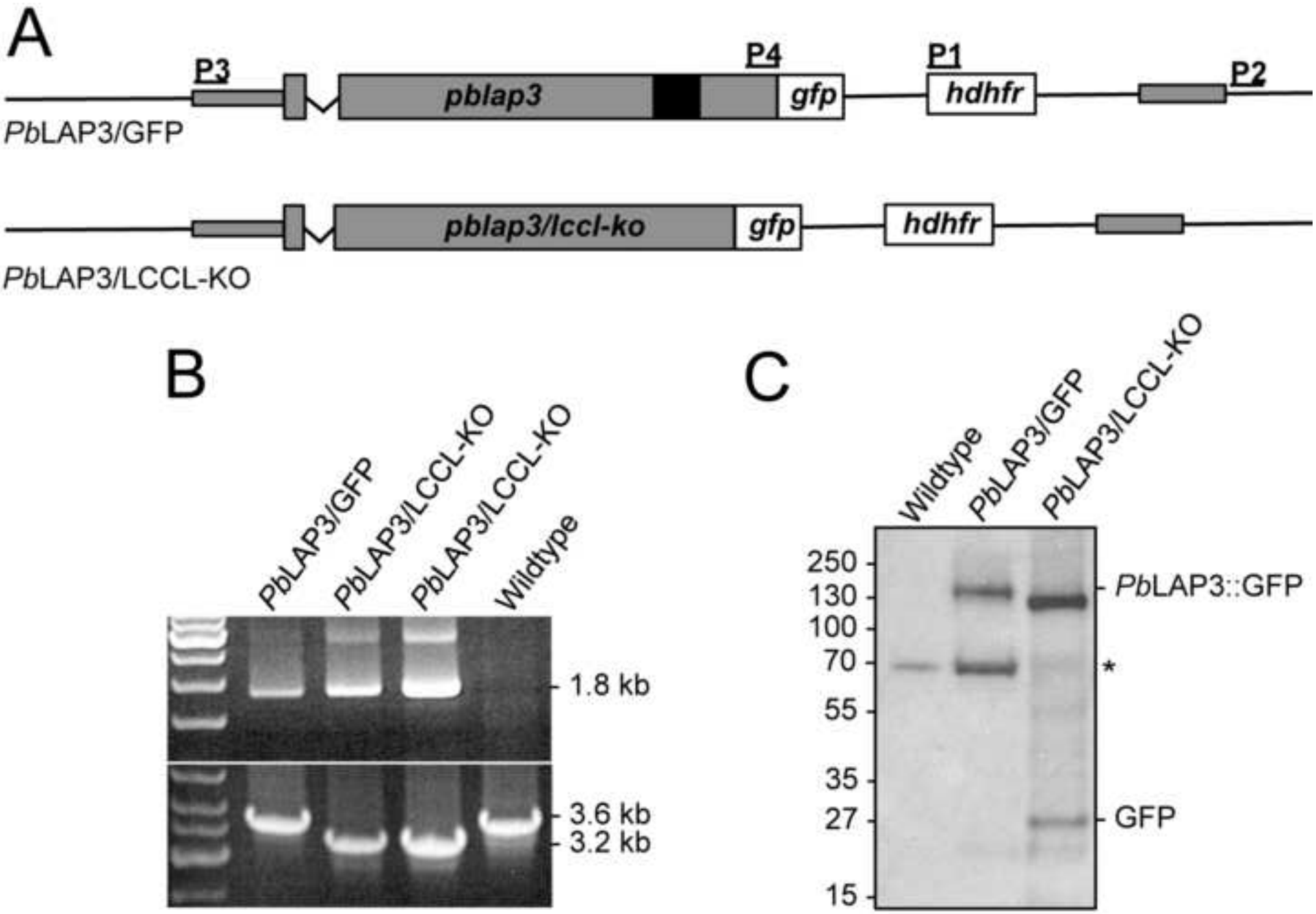

Figure 3

Click here to download high resolution image

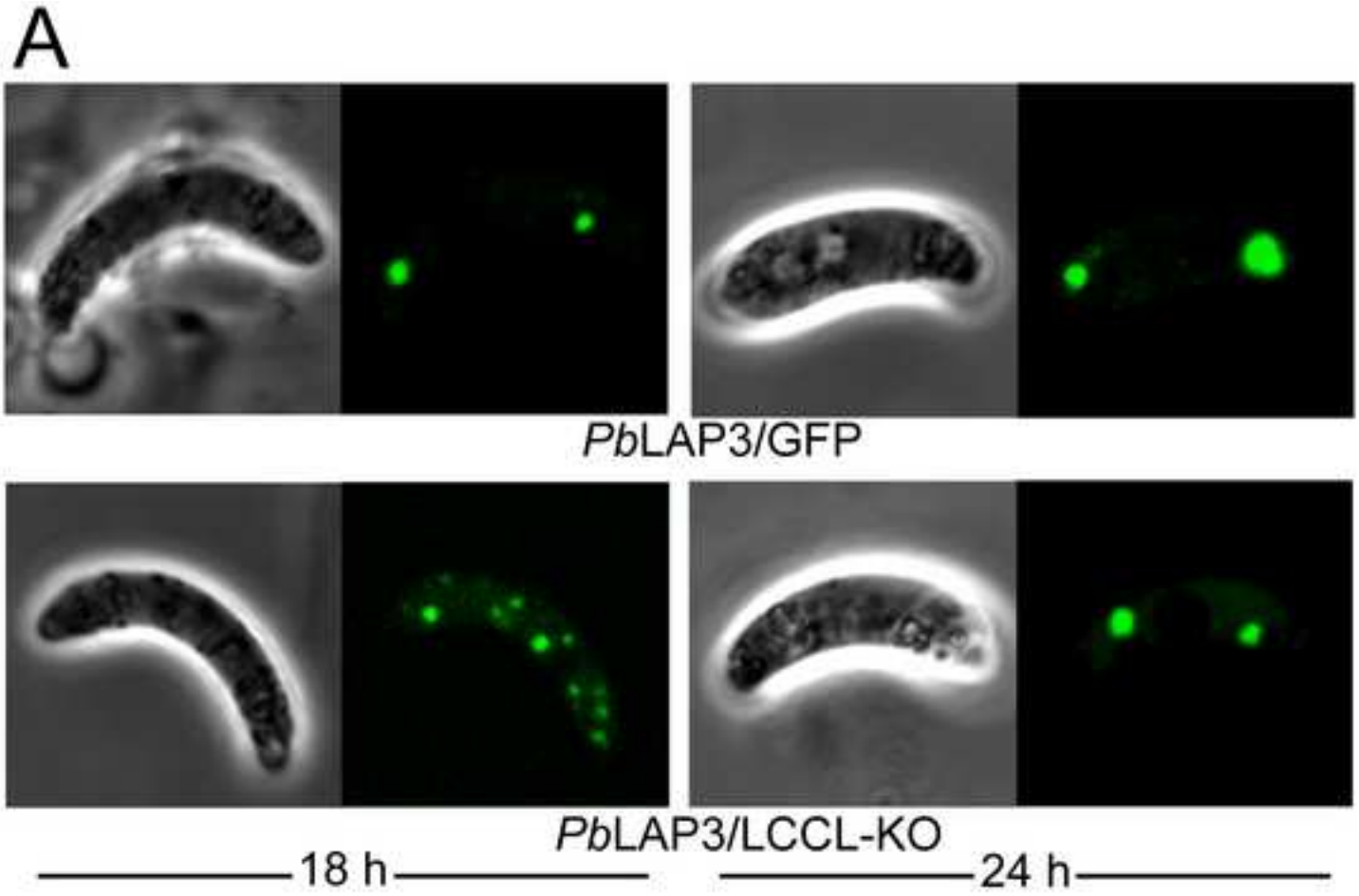

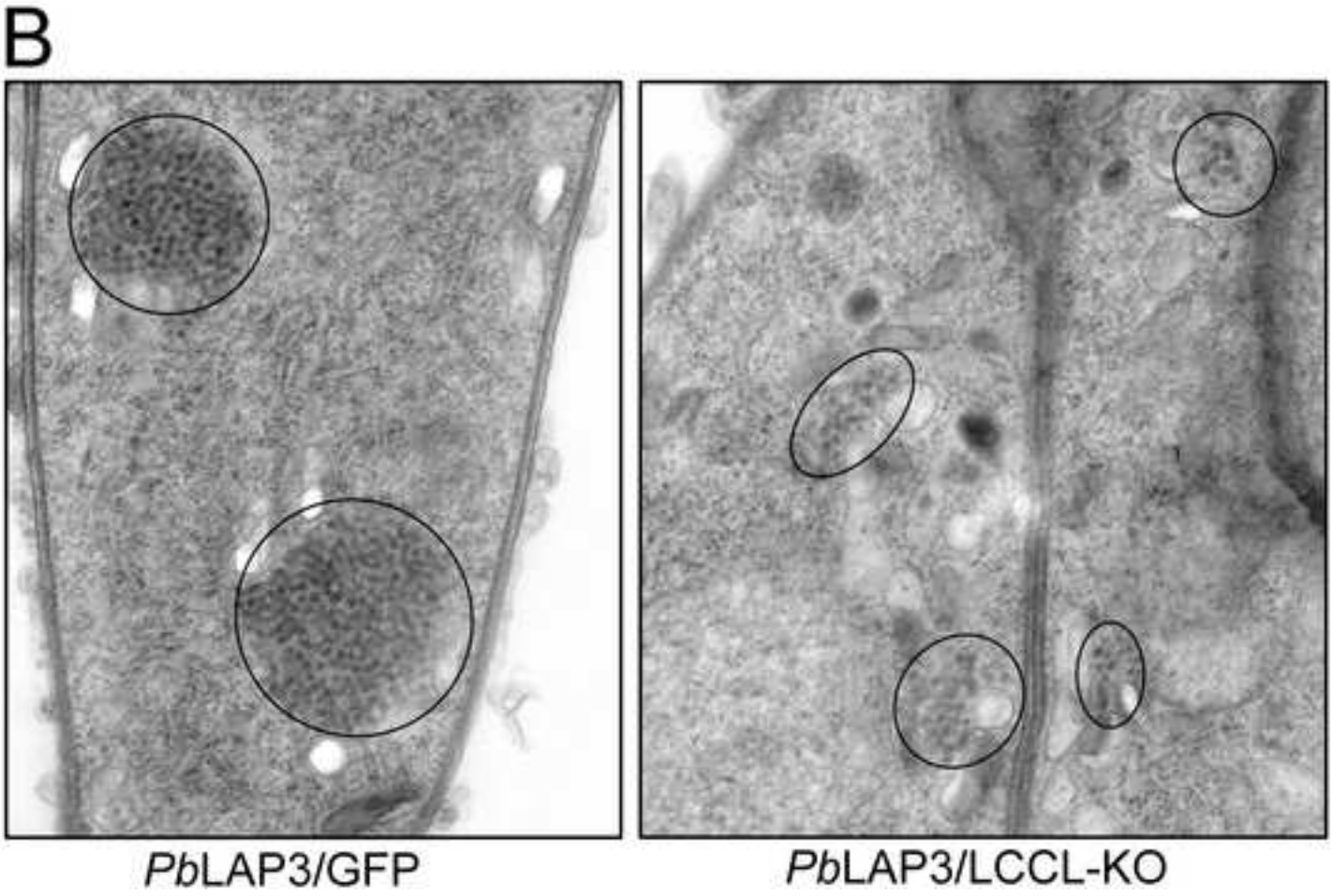

Figure 4

Click here to download high resolution image

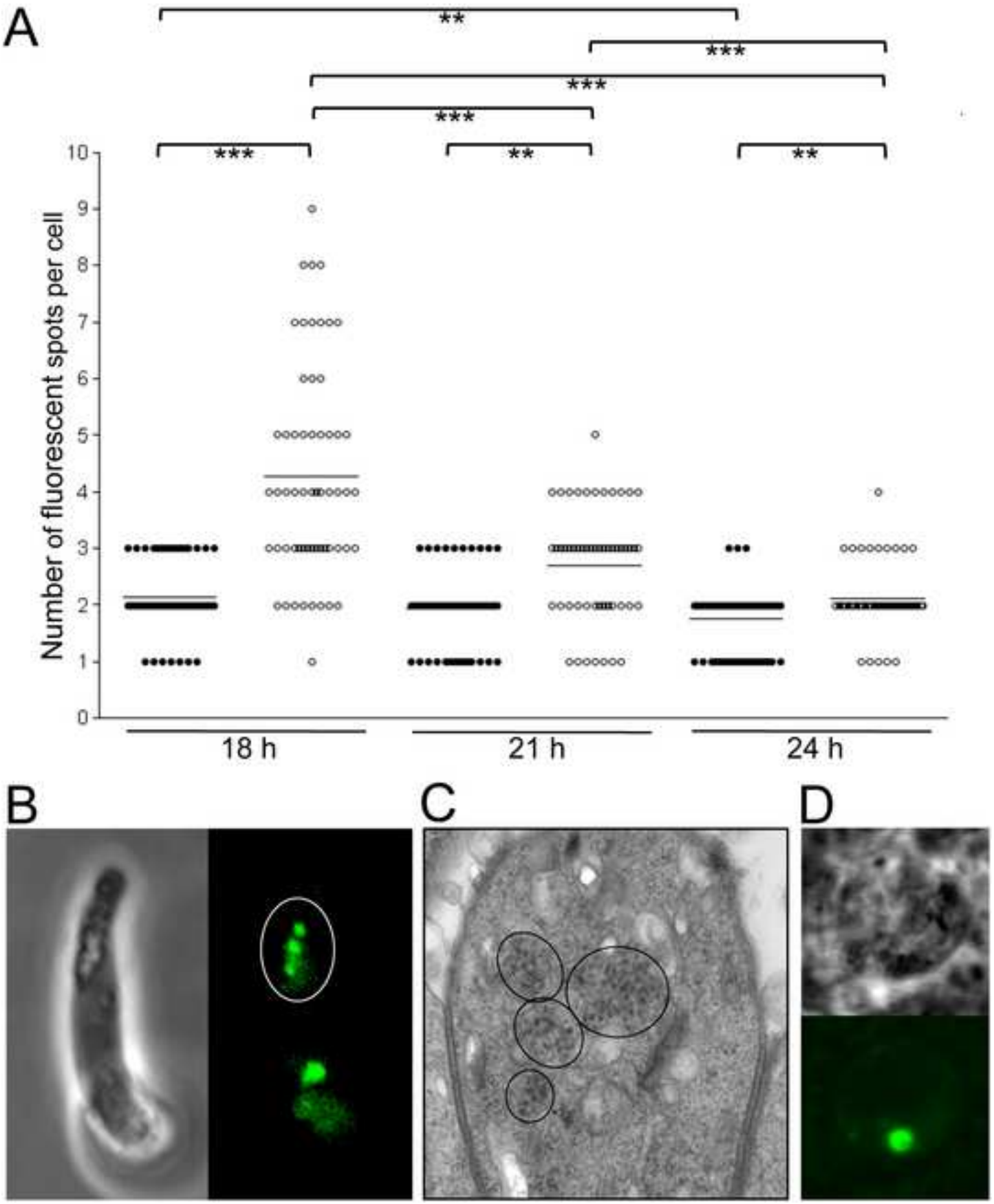

Figure 5

Click here to download high resolution image

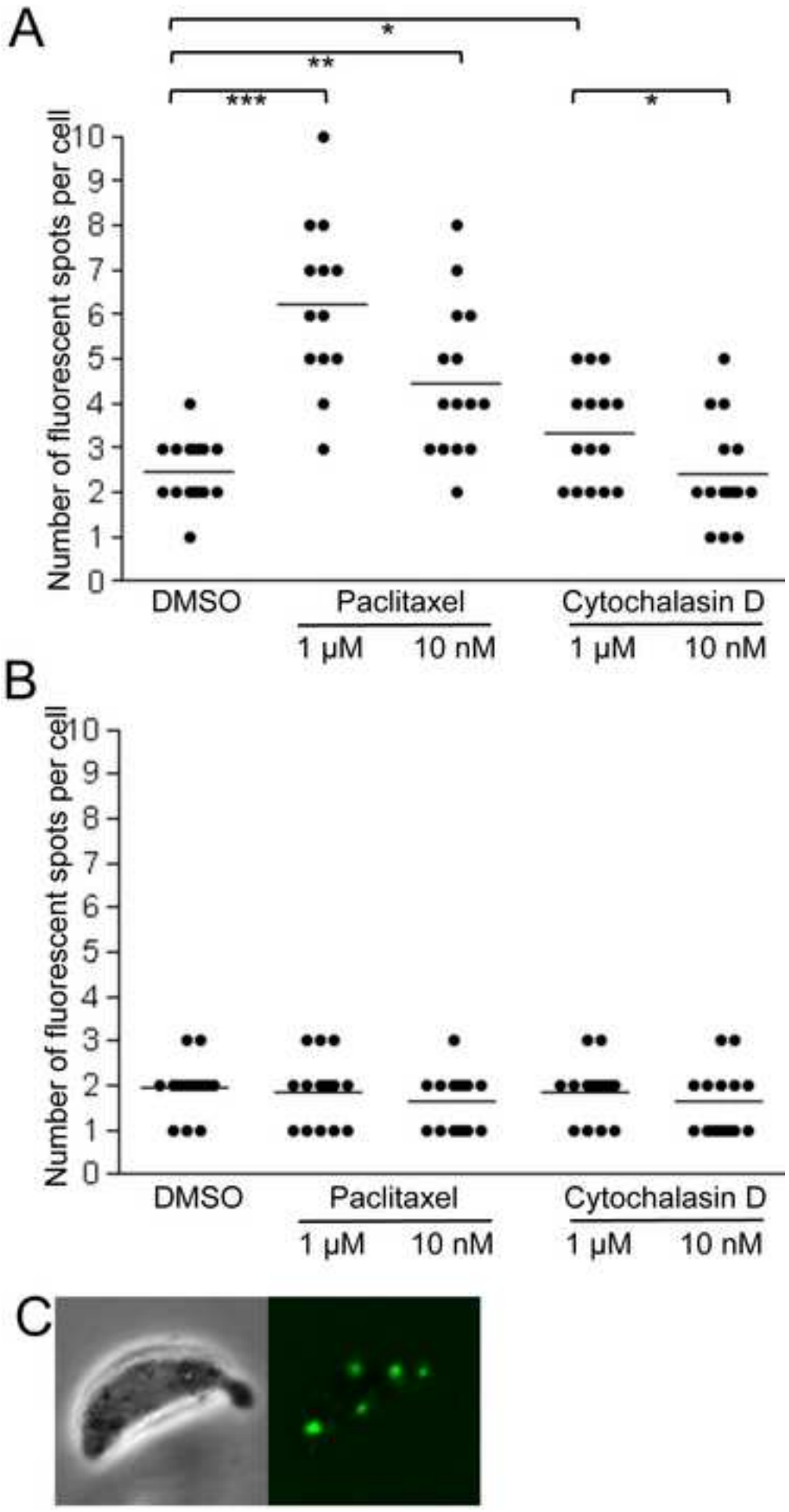

Figure 6

Click here to download high resolution image

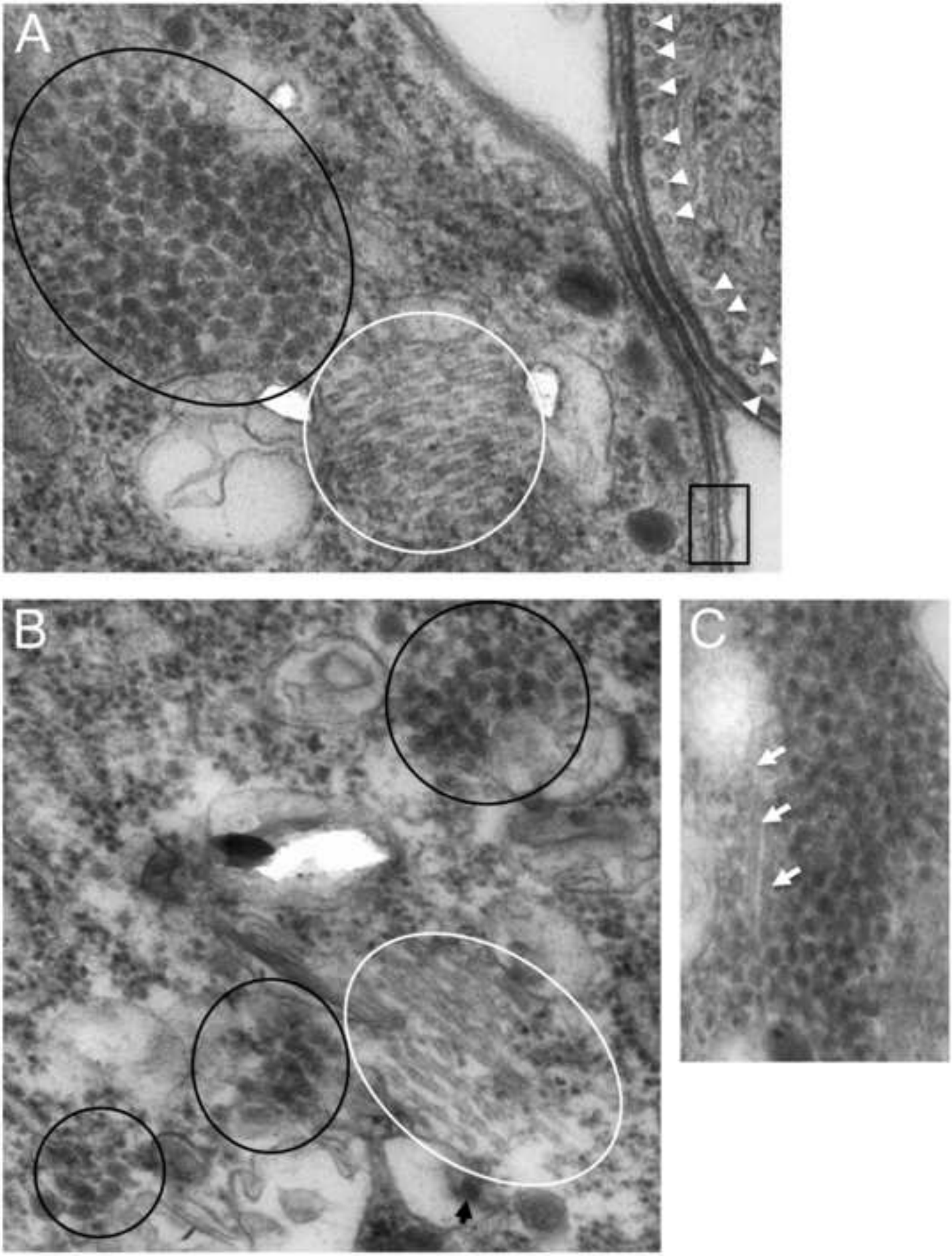

Figure 7

Click here to download high resolution image

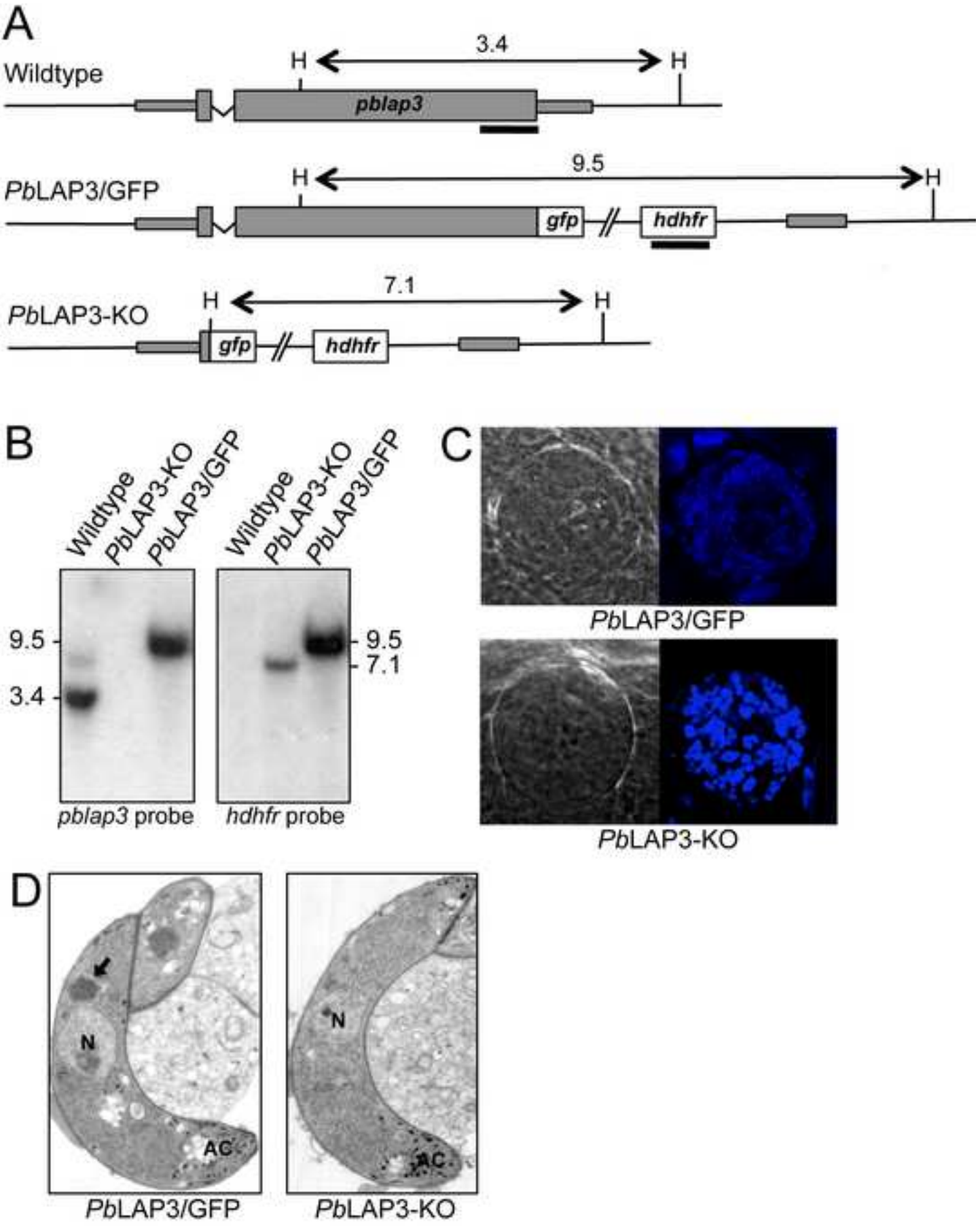

Figure 8

Click here to download high resolution image